

365. Investigation of vibrations of packaging materials

E. Kibirkštis¹, A. Kabelkaitė¹, A. Dabkevičius¹, L. Ragulskis²

¹Kaunas University of Technology,
Studentų 56-350, LT-51424 Kaunas, Lithuania,

Tel.: (8 37) 300 237,

E-mail: *edmundas.kibirkstis@ktu.lt, asta.kabelkaite@ktu.lt, arturas.dabkevicius@ktu.lt*

²Vytautas Magnus University,
Vileikos 8-702, LT-44404 Kaunas, Lithuania,

E-mail: *l.ragulskis@if.vdu.lt*

(Received 24 March 2008; accepted 13 June 2008)

Abstract. The stress strain law on the basis of the model of a visco-elastic body is proposed. Procedure for numerical integration of equations of motion is developed. Results of numerical calculations of vibrations of a visco-elastic structure are presented.

It is assumed that a paper in a printing device is loaded in its plane and thus a problem of plane stress is analyzed. The principal stresses are calculated and represented at the centers of finite elements. They substantially determine the vibration behavior and stability of the polymeric film.

The first eigenmodes are presented for a paper performing transverse vibrations as a plate having additional stiffness due to static tension in its plane.

Stresses in the polymeric film in the transverse and longitudinal direction of transportation of the tape were determined by using experimental methods for the symmetric and non-symmetric loads. For the investigation of the eigenmodes a special experimental setup was used in which the eigenmodes of the paper tape were determined by using the method of projection moire under the action of vibrations to the tape of paper for the symmetric load. Comparison of the experimental and numerical results of investigation was performed.

Keywords: visco-elasticity, stress strain law, modal equations, numerical integration, finite elements, polymeric film, paper, plane stress, principal stresses, vibrations, eigenmode, plate, experimental setup, stress measurement, projection moire.

Introduction

The stress strain law on the basis of the model of a visco-elastic body described in [1] is proposed. Modal decomposition of the equations of motion by using the eigenproblem of an un-damped system [2, 3, 4] is performed. Procedure for numerical integration of the modal equations is developed. Results of numerical calculations of vibrations of a visco-elastic structure are presented.

The model for the analysis of a paper in a printing device is proposed on the basis of the material described in [3, 4]. It is assumed that a paper in a printing device is loaded in its plane. Thus the static problem of plane stress by assuming the displacements at the boundary of the analyzed paper to be given is solved.

The principal stresses are calculated and represented at the centers of finite elements. They substantially determine the vibration behavior and stability of the polymeric film.

The analysis of vibrations of a paper in a printing device is performed on the basis of the model

described in [5]. The investigation presented here is the continuation of the previous analysis given in [5, 6].

Stresses in the polymeric film in the transverse and longitudinal direction of transportation of the tape were determined by using experimental methods for the symmetric and non-symmetric loads.

For the investigation of the eigenmodes a special experimental setup was used in which the eigenmodes of the paper tape were determined by using the method of projection moire under the action of vibrations to the tape of paper for the symmetric load. Comparison of the experimental and numerical results of investigation was performed.

Model for the analysis of vibrations of a polymeric film

The stress strain law on the basis of the model of a visco-elastic body [1] is assumed in the following form:

$$\{\sigma\} = [D]\{\varepsilon\} + \beta[D]\{\dot{\varepsilon}\} - \gamma\{\dot{\sigma}\}, \quad (1)$$

where $\{\sigma\}$ is the stress vector, $\{\varepsilon\}$ is the strain vector, $[D]$ is the matrix of elastic constants, β is the coefficient of internal damping, γ is the relaxation time and the upper dot denotes differentiation with respect to time.

It is assumed that:

$$|\beta| \ll 1, \tag{2}$$

And

$$|\gamma| \ll 1. \tag{3}$$

By taking into account the products of β and γ up to the fourth power the stress strain law is expressed as:

$$\begin{aligned} \{\sigma\} = & [D]\{\varepsilon\} + (\beta - \gamma)[D]\{\dot{\varepsilon}\} + \gamma(\gamma - \beta)[D]\{\ddot{\varepsilon}\} + \\ & + \gamma^2(\beta - \gamma)[D]\{\ddot{\varepsilon}\} + \gamma^3(\gamma - \beta)[D]\{\varepsilon\}. \end{aligned} \tag{4}$$

The equation of motion takes the form:

$$\begin{aligned} \gamma^3(\gamma - \beta)[K]\{\delta\} + \gamma^2(\beta - \gamma)[K]\{\delta\} + \\ + [[M] + \gamma(\gamma - \beta)[K]]\{\dot{\delta}\} + \\ + [\alpha[M] + (\beta - \gamma)[K]]\{\delta\} + [K]\{\delta\} = \{F\}, \end{aligned} \tag{5}$$

Where $[K]$ and $[M]$ are the symmetric and positive definite stiffness and mass matrices of the elastic structure, $\{\delta\}$ is the displacement vector, $\{F\}$ is the loading vector and α is the coefficient of external damping.

The eigenproblem is solved [2, 3, 4]:

$$([K] - \omega_i^2[M])\{\delta_i\} = \{0\}, \tag{6}$$

which determines the eigenfrequencies ω_i and the eigenmodes $\{\delta_i\}$. The eigenmodes satisfy the conditions [2, 3, 4]:

$$\{\delta_i\}^T [M] \{\delta_j\} = \begin{cases} 1, & \text{when } i = j, \\ 0, & \text{when } i \neq j, \end{cases} \tag{7}$$

and

$$\{\delta_i\}^T [K] \{\delta_j\} = \begin{cases} \omega_i^2, & \text{when } i = j, \\ 0, & \text{when } i \neq j. \end{cases} \tag{8}$$

The motion is expressed as [2, 3, 4]:

$$\{\delta\} = [\{\delta_1\} \ \{\delta_2\} \ \dots] \begin{Bmatrix} z_1 \\ z_2 \\ \vdots \end{Bmatrix}, \tag{9}$$

where z_1, z_2, \dots are the modal decomposition coefficients.

Thus the modal equations have the following form:

$$\begin{aligned} \gamma^3(\gamma - \beta)\omega_i^2 \ddot{z}_i + \gamma^2(\beta - \gamma)\omega_i^2 \dot{z}_i + \\ + (1 + \gamma(\gamma - \beta)\omega_i^2)\ddot{z}_i + (\alpha + (\beta - \gamma)\omega_i^2)\dot{z}_i + \\ + \omega_i^2 z_i = \{\delta_i\}^T \{F\}. \end{aligned} \tag{10}$$

Integration of the modal equations of a polymeric film

The modal equation has the form:

$$b \ddot{x} + a\dot{x} + m\ddot{x} + c\dot{x} + kx = f, \tag{11}$$

where b, a, m, c, k are constants, f and x are functions of time.

The constant average acceleration of acceleration procedure of Newmark type is based on the relationships:

$$\ddot{x}_T = \ddot{x}_0 + \left(\overset{\dots}{x_0} + \overset{\dots}{x_T} \right) \frac{T}{2}, \tag{12}$$

$$\dot{x}_T = \dot{x}_0 + \ddot{x}_0 T + \left(\overset{\dots}{x_0} + \overset{\dots}{x_T} \right) \frac{T^2}{4}, \tag{13}$$

$$x_T = x_0 + \dot{x}_0 T + \ddot{x}_0 \frac{T^2}{2} + \left(\overset{\dots}{x_0} + \overset{\dots}{x_T} \right) \frac{T^3}{12}, \tag{14}$$

$$\begin{aligned} x_T = x_0 + \dot{x}_0 T + \ddot{x}_0 \frac{T^2}{2} + \overset{\dots}{x}_0 \frac{T^3}{6} + \\ + \left(\overset{\dots}{x_0} + \overset{\dots}{x_T} \right) \frac{T^4}{48}, \end{aligned} \tag{15}$$

where T is the time step and the subscript indicates the moment of time. Acceleration of acceleration is determined from:

$$\begin{aligned} \left(b + a \frac{T}{2} + m \frac{T^2}{4} + c \frac{T^3}{12} + k \frac{T^4}{48} \right) \overset{\dots}{x}_T = f - \\ - k \left(x_0 + \dot{x}_0 T + \ddot{x}_0 \frac{T^2}{2} + \overset{\dots}{x}_0 \frac{T^3}{6} + \right. \\ \left. + \overset{\dots}{x}_0 \frac{T^4}{48} \right) - \\ - c \left(\dot{x}_0 + \ddot{x}_0 T + \overset{\dots}{x}_0 \frac{T^2}{2} + \overset{\dots}{x}_0 \frac{T^3}{12} \right) - \\ - m \left(\ddot{x}_0 + \overset{\dots}{x}_0 T + \overset{\dots}{x}_0 \frac{T^2}{4} \right) - a \left(\overset{\dots}{x}_0 + \overset{\dots}{x}_0 \frac{T}{2} \right). \end{aligned} \tag{16}$$

Results of the analysis of vibrations of a polymeric film

An axi-symmetric problem is analyzed. A thin square structure is parallel to the axial coordinate. On the lower boundary all the displacements are assumed equal to zero. The central node on the upper boundary is loaded in the direction of the axial coordinate.

The time history of loading is shown in Fig. 1. The time history of motion of the loaded degree of freedom for the un-damped system is shown in Fig. 2, for the system with external damping it is shown in Fig. 3, for the system with internal damping it is shown in Fig. 4, for the system with internal damping and relaxation it is shown in Fig. 5.

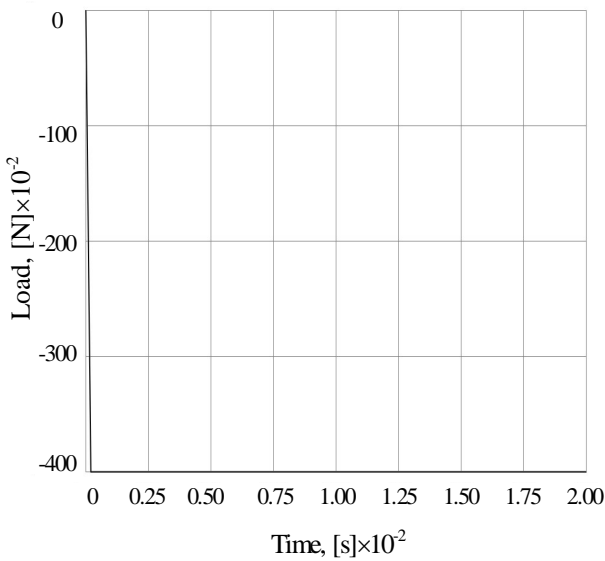


Fig. 1. The time history of loading

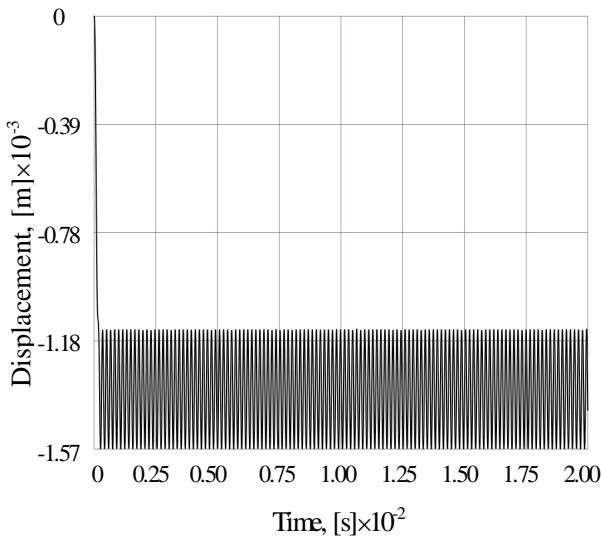


Fig. 2. The time history of motion for the un-damped system

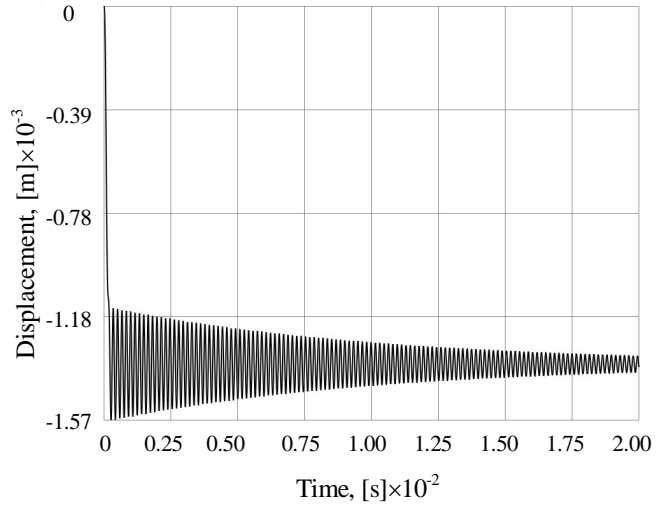


Fig. 3. The time history of motion for the system with external damping

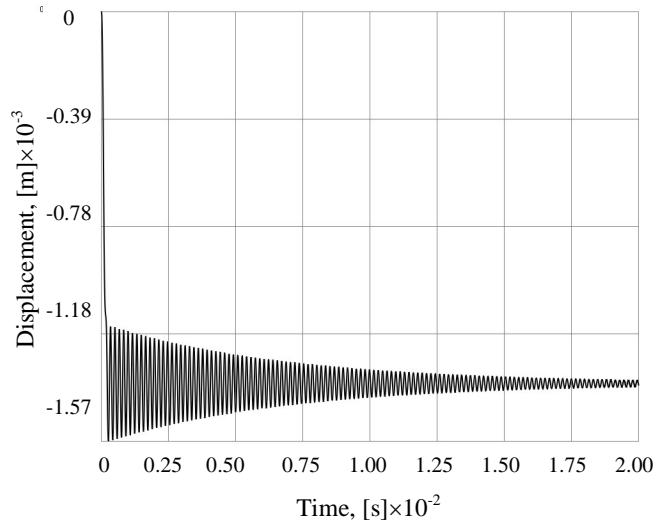


Fig. 4. The time history of motion for the system with internal damping

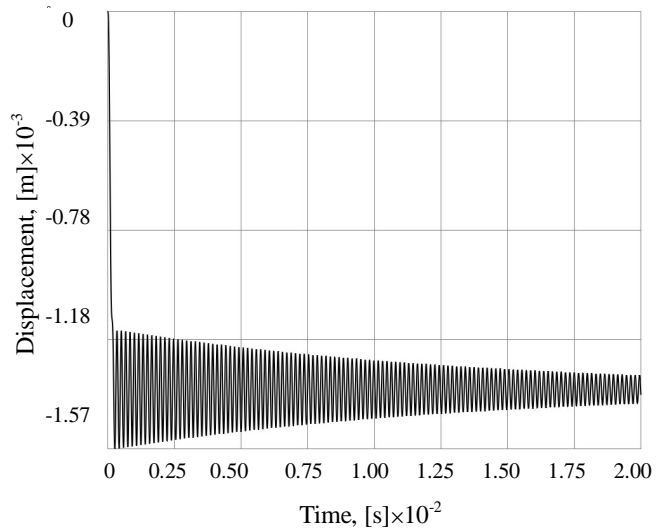


Fig. 5. The time history of motion for the system with internal damping and relaxation

Procedure of analysis of stresses in the polymeric film in a printing device

Further x and y denote the axes of the orthogonal Cartesian system of coordinates. The static problem of plane stress is analyzed. The element has two nodal degrees of freedom: the displacements u and v in the directions of the axes x and y of the orthogonal Cartesian system of coordinates.

It is assumed that the displacements at the boundary of the analyzed polymeric film are given and they produce the loading vector. Thus the vector of displacements is determined by solving the system of linear algebraic equations.

The stresses σ_x , σ_y , τ_{xy} are determined at the centers of the finite elements from this static problem of plane stress. The principal stresses are calculated and their directions are represented inside the smaller circle, while their values are proportional to the black angle between the two circles. One drawing is produced for the representation of positive values and another drawing is produced for the representation of negative values.

Results of analysis of stresses under symmetric and un-symmetric loading of the polymeric film in a printing device

The square piece of paper is analyzed. The following boundary conditions are assumed: on the lower boundary it is assumed that $u=v=0$; on the upper boundary it is assumed that $u=0$ and $v=1$.

In this problem the principal stresses at the centers of finite elements are everywhere positive and are presented in Fig. 6.

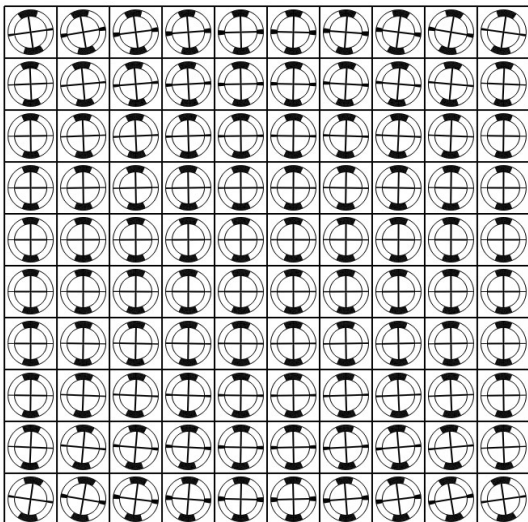


Fig. 6. The principle stresses under symmetric loading

The same piece of paper is analyzed, but on the upper boundary linear variation of the displacement v is assumed with $v=0.5$ on the left side of the boundary and $v=1.5$ on the right side of the boundary.

The values of positive principal stresses at the centers of finite elements are presented in Fig. 7, while the values of negative principal stresses at the centers of finite elements are presented in Fig. 8. The values of negative principle stresses are much smaller than the values of positive principle stresses. So the scale for the representation of the values of negative principle stresses is two hundred times more sensitive than for the values of positive principle stresses.

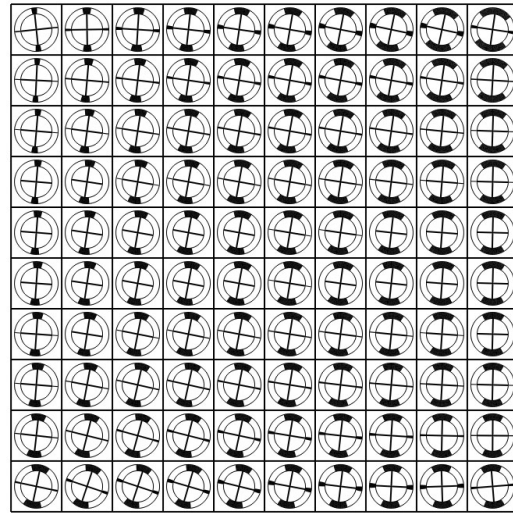


Fig. 7. The values of positive principle stresses under un-symmetric loading

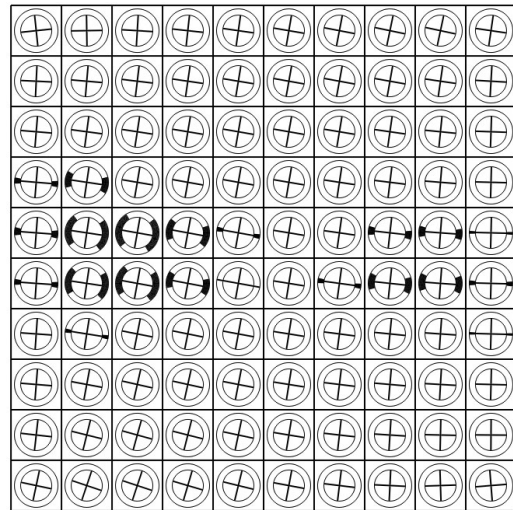


Fig. 8. The values of negative principle stresses under un-symmetric loading

The stresses in the plane of the polymeric film substantially influence the bending stiffness of the polymeric film and thus its transverse vibrations. In the regions where there is a negative principle stress the loss of stability of the polymeric film can be expected.

Experimental investigation of stresses of the tape of polymeric film

In some cases it may happen that in the circular printing device the tape of the polymeric film may have an un-symmetric loading of the film with respect to the direction of the cylindrical surface of the circular element because of the change of direction and bending of the directing circular elements. This may take place because of the incorrect mounting of supports of the directing circular elements of the tape, the wear of bearings and other reasons.

In order to evaluate the distribution of normal stresses of a flexible polymeric tape when the printing material is being transported under the action of symmetric and un-symmetric loads the setup for experimental investigation was designed and produced (Fig. 9a).

The normal stresses (σ_x and σ_y) in the flexible polymeric film were measured by using a tensometric sensor at definite points of the investigated region in two mutually perpendicular directions (in the longitudinal and transverse directions of the polymeric tape) according to the diagram presented in Fig. 9b).

For the case of un-symmetric loading of the tape of the film the load was distributed un-symmetrically in the transverse direction of the tape of the polymeric film, one of its sides being loaded more than the other side. The diagrams of symmetric and un-symmetric ways of loading are presented in Fig. 9c and Fig. 9d.

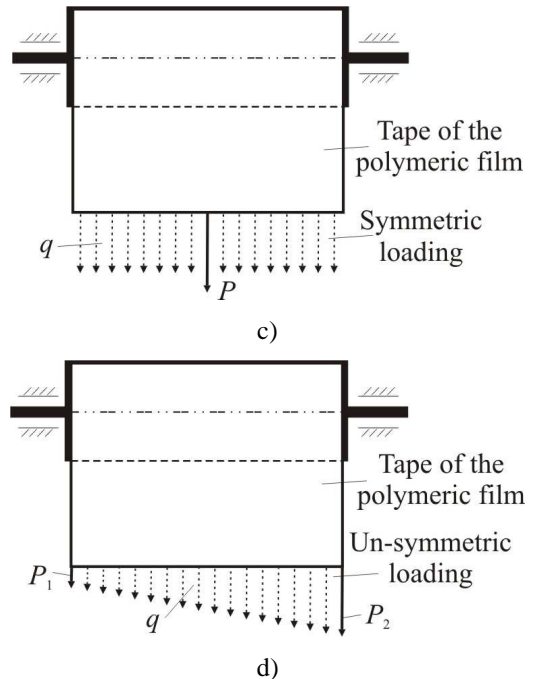
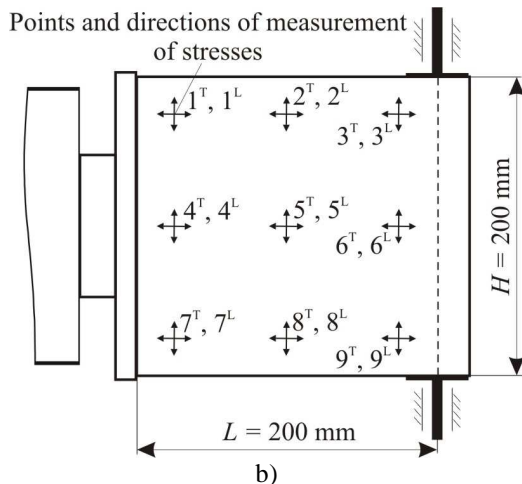
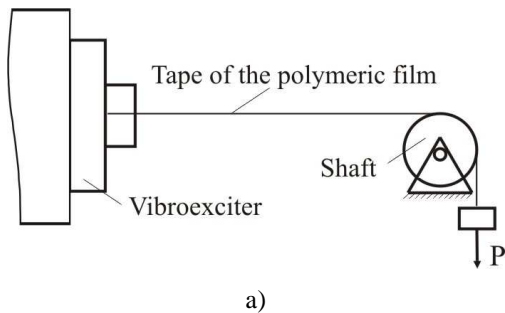


Fig. 9. Setup for experimental investigation of the stresses in the polymeric film: a) general view of the experimental setup: P – loading force; b) diagram of measurement of stresses in the tape, points and directions of measurements: 1...9 – number of position for measurement of stresses; S – transverse direction of stress measurement; I – longitudinal direction of measurement; c) symmetric way of loading of a polymeric film: q – loading, P – loading force; d) un-symmetric way of loading: q – loading, P_1 and P_2 – loading forces

The measurements of stresses in the defined points of the tape were performed no less than three times each and from the obtained data the arithmetic mean values were obtained. According to the obtained results the graphical relationships of the distribution of stresses of the polymeric film POP+AL+LDPE were drawn. On the basis of those relationships it is possible to make conclusions about the character of distribution of stresses in the tape.

The results of measurements of the obtained normal stresses are presented in the graphical relationships of Fig. 10 and Fig. 11.

From Fig. 10 one can observe that the stresses in the analyzed region of the polymeric film are distributed unevenly. Moreover the values of stresses changes depending on the direction of measurement and the value of the applied loading force. The highest values of stresses occur when the direction of measurement coincides with the direction of loading (the measurements are performed in the direction parallel to the direction of loading). In this case maximum stresses are obtained at point 4: the stresses $\sigma_x = 3,56$ MPa, when the loading force $P = 14,72$ N. When the direction of measurement is parallel to the direction of loading, the stresses become smaller with the increase of loading. The stresses at the same point 4 are obtained smaller $\sigma_x = 3,28$ MPa, when the loading force $P = 19,62$ N. When the

measurements are performed parallel to the direction of loading the smallest stresses take place at point 5: $\sigma_x = 3,2$ MPa, when the loading force $P = 14,72$ N, and $\sigma_x = 2,92$ MPa, when the loading force $P = 19,62$ N.

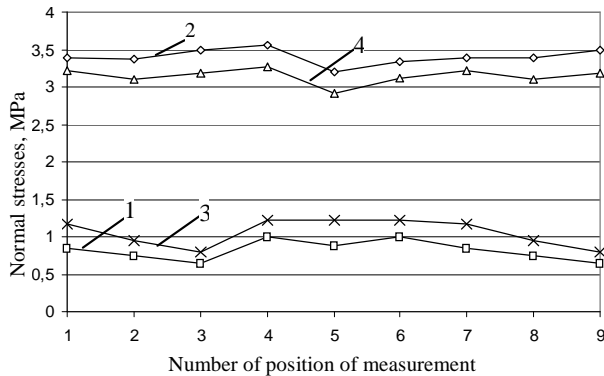


Fig. 10. Graphical relationships of the distribution of stresses of the multilayered polymeric film POP+AL+LDPE in the tape of the polymeric film for symmetric loading: 1 – the stresses σ_y , for the symmetric loading force $P = 14,72$ N, when the direction of measurement is perpendicular to the direction of loading; 2 – the stresses σ_x , for the symmetric loading force $P = 14,72$ N, when the direction of measurement is parallel to the direction of loading; 3 – the stresses σ_y , for the symmetric loading force $P = 19,62$ N, when the direction of measurement is perpendicular to the direction of loading; 4 – the stresses σ_x , for the symmetric loading force $P = 19,62$ N, when the direction of measurement is parallel to the direction of loading

From Fig. 10 one can observe that when the direction of measurement is perpendicular to the direction of loading of the polymeric film, then the stresses become smaller when going further from the place of fixing of the polymeric film: compare $\sigma_{y1} = 1,17$ MPa, $\sigma_{y2} = 0,94$ MPa and $\sigma_{y3} = 0,79$ MPa, when the loading force $P = 19,62$ N. Also one can observe that when the direction of measurement is perpendicular to the direction of loading of the polymeric film, with the increase of loading the stresses increase (contrary to the case when the direction of measurement is parallel to the direction of loading): at point 1: $\sigma_y = 0,84$ MPa, when the loading force $P = 14,72$ N, and $\sigma_y = 1,17$ MPa, when the loading force $P = 19,62$ N.

In Fig. 11 the stresses and their distribution in a multilayered polymeric film POP+AL+LDPE are presented for the un-symmetric load.

From Fig. 11 one can observe that the highest stresses take place, as in the previously analyzed case, at point 4 (when the direction of measurement coincides with the direction of loading): the stresses $\sigma_x = 3,39$ MPa, when the loading forces $P_1 = 14,72$ N and $P_2 = 19,62$ N. For this case of un-symmetric loading when the direction of measurement is parallel to the direction of loading, the stresses become smaller with the increase of load, but not so much smaller as in the previously analyzed case of symmetric loading: for example at

point 3 the stresses $\sigma_x = 2,92$ MPa, when the loading forces $P_1 = 14,72$ N and $P_2 = 19,62$ N, and $\sigma_x = 2,66$ MPa, when the loading forces increase ($P_1 = 19,62$ N and $P_2 = 24,52$ N).

For the case of un-symmetric loading when the direction of measurement is perpendicular to the direction of loading of the polymeric film, the stresses σ_y become smaller when going further from the place of fixing of the polymeric film on that side of the film at which the loading force P_2 is larger: compare $\sigma_{y7} = 0,79$ MPa, $\sigma_{y8} = 0,73$ MPa and $\sigma_{y9} = 0,67$ MPa, when the loading forces are $P_1 = 14,72$ N and $P_2 = 19,62$ N. At the same time on the other side of the film (where the load is smaller) the character of variation of stresses is not so evident: $\sigma_{y1} = 1,61$ MPa, $\sigma_{y2} = 1,48$ MPa and $\sigma_{y3} = 1,34$ MPa, when the loading forces are $P_1 = 19,62$ N and $P_2 = 24,52$ N.

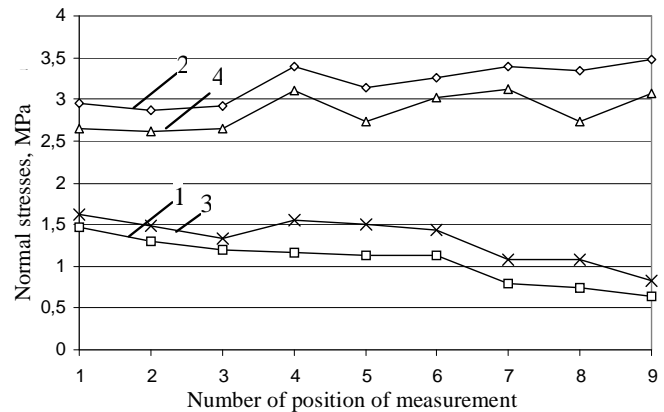


Fig. 11. Graphical relationships of the distribution of stresses of the multilayered polymeric film POP+AL+LDPE in the tape of the polymeric film for un-symmetric loading: 1 – the stresses σ_y , for the loading forces $P_1 = 14,72$ N and $P_2 = 19,62$ N, when the direction of measurement is perpendicular to the direction of loading; 2 – the stresses σ_x , for the loading forces $P_1 = 14,72$ N and $P_2 = 19,62$ N, when the direction of measurement is parallel to the direction of loading; 3 – the stresses σ_y , for the loading forces $P_1 = 19,62$ N and $P_2 = 24,52$ N, when the direction of measurement is perpendicular to the direction of loading; 4 – the stresses σ_x , for the loading forces $P_1 = 19,62$ N and $P_2 = 24,52$ N, when the direction of measurement is parallel to the direction of loading

Also one can see that when the direction of measurement is perpendicular to the direction of loading of the polymeric film, with the increase of load the stresses σ_y increase (in a similar way as in the previously analyzed case): at point 1: $\sigma_y = 1,47$ MPa, when the loading forces $P_1 = 14,72$ N and $P_2 = 19,62$ N, and $\sigma_y = 1,62$ MPa, when the loading forces $P_1 = 19,62$ N and $P_2 = 24,52$ N.

It is seen that the experimental data corresponds to the numerical investigations: for the case of symmetric loading Fig. 6 and Fig. 10, and for the case of un-symmetric loading Fig. 7, Fig. 8 and Fig. 11.

Results of analysis of vibrations of the paper in a printing device

The square piece of paper is analyzed. For the static problem of plane stress the following boundary conditions

are assumed: on the lower boundary it is assumed that $u=v=0$; on the upper boundary it is assumed that $u=0$ and $v=1$. For the problem of transverse vibrations on the lower and upper boundaries all the generalized displacements are assumed equal to zero.

Contour plot of the transverse displacement for the first eigenmode is presented in Fig. 12, for the second eigenmode in Fig. 13, ... , for the ninth eigenmode in Fig. 20.

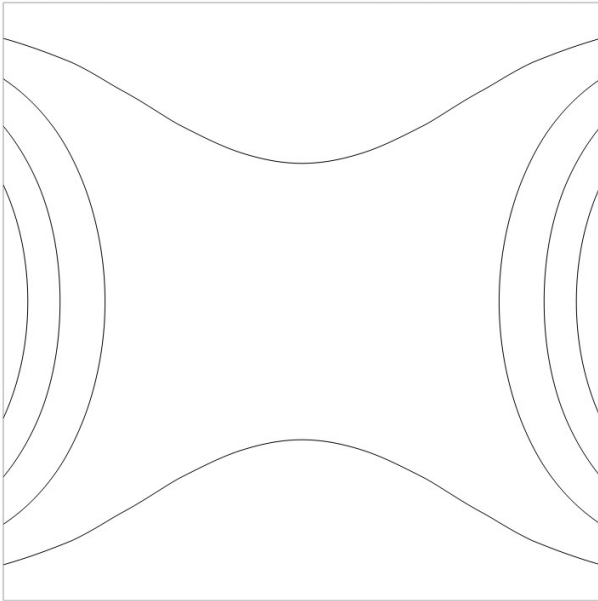


Fig. 12. The first eigenmode

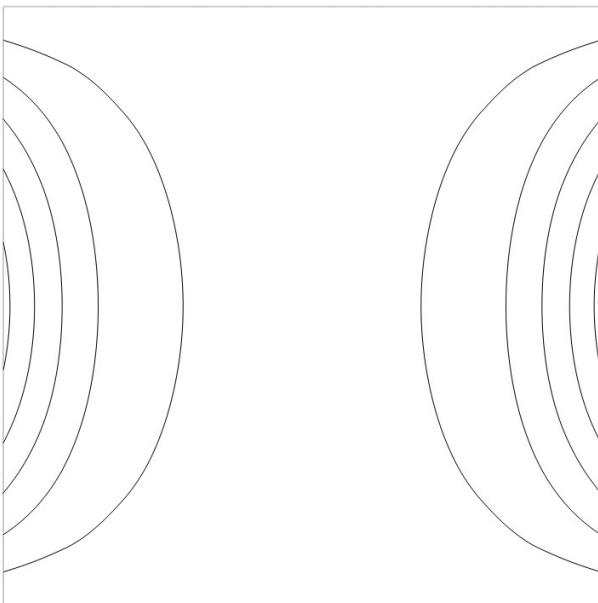


Fig. 13. The second eigenmode

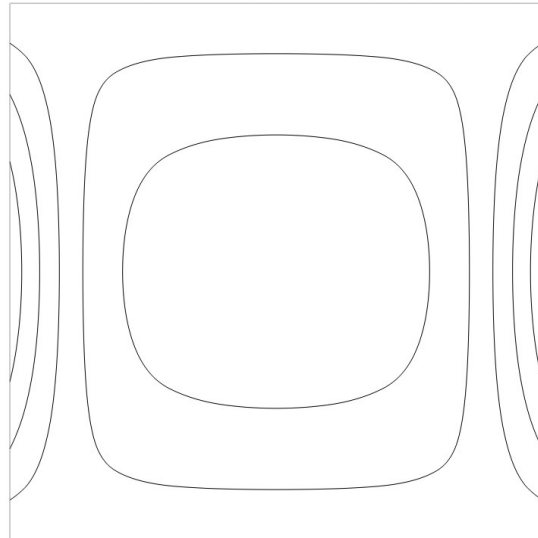


Fig. 14. The third eigenmode

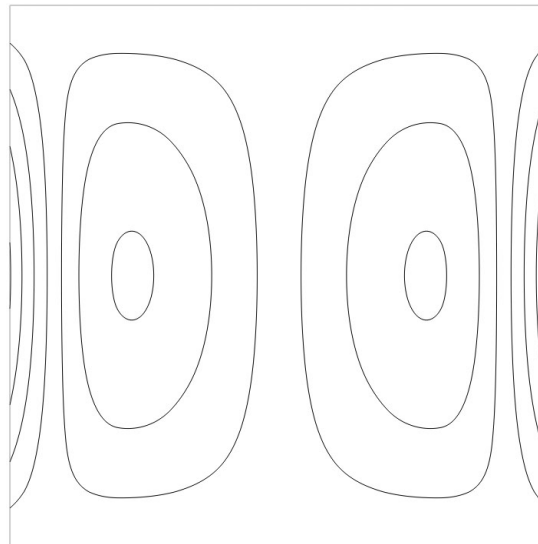


Fig. 15. The fourth eigenmode

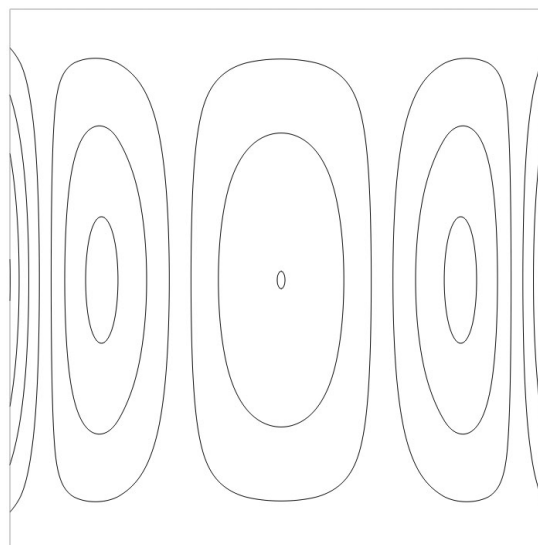


Fig. 16. The fifth eigenmode

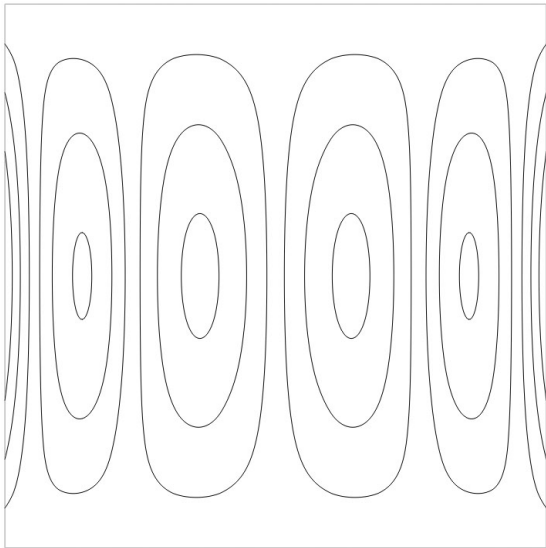


Fig. 17. The sixth eigenmode

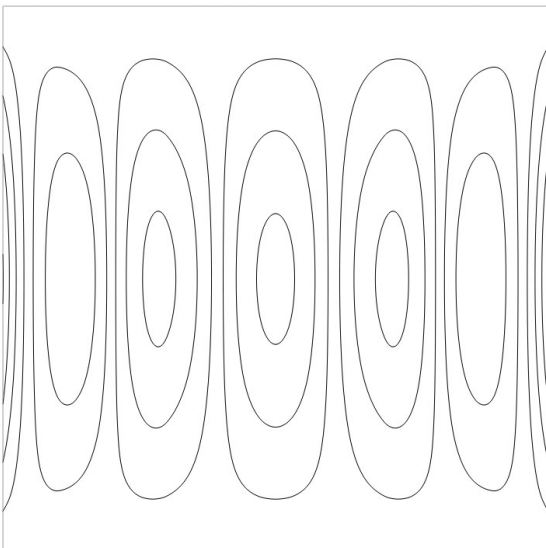


Fig. 18. The seventh eigenmode

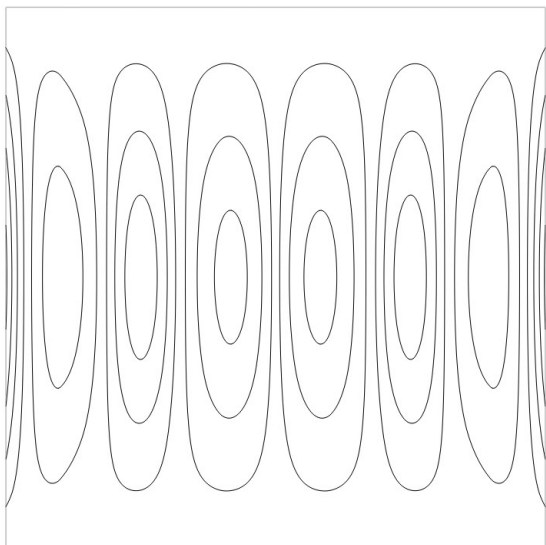


Fig. 19. The eighth eigenmode

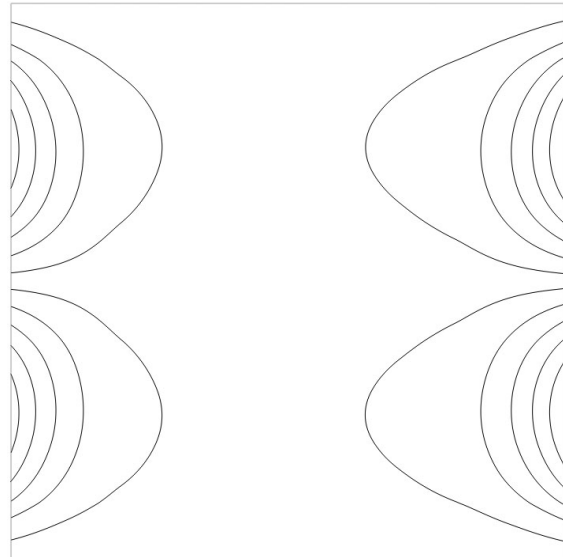


Fig. 20. The ninth eigenmode

Analysis of results of experimental and numerical investigations of vibrations of a paper tape

In the same way as in the previous papers [5, 6] the eigenmodes of the paper tape were investigated by using a specially designed experimental setup, which structural diagram is illustrated in Fig. 21. The investigated material was loaded symmetrically by the force P (25,5 N). The exciter of vibrations was used for the generation of longitudinal vibrations of sinusoidal shape of the chosen frequency, which excited standing waves in the material tape. For the visualization of eigenmodes the grid of step p was projected at a definite angle on the surface of the investigated material by the flux of light emitted from a source of monochromatic light [5, 6]. The eigenmodes obtained by using the method of experimental investigation were registered by a digital camera and observed in the monitor of a personal computer.

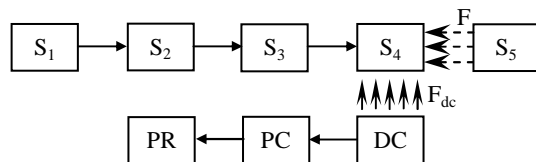


Fig. 21. Structural diagram of the setup for experimental investigation: S_1 – signal generator; S_2 – signal amplifier; S_3 – vibroexciter; S_4 – the investigated material; S_5 – source of monochromatic light; DC – digital camera; PC – personal computer; PR – printer; F_{dc} – light flux of the digital camera; F – light flux projected by a source of monochromatic light.

The experiments were conducted by using the chalk mate Luxo Satin 300 g/m² paper, exciting it by longitudinal vibrations of sinusoidal shape of chosen frequency in the cross-machine direction of paper. Technical characteristics of

this paper are presented in Table 1. For the samples of the investigated material the square list of paper 20×20 cm was used.

Table 1. Technical characteristics of the chalk paper Luxo Satin

Qualities	Luxo Satin
Grammage, g/m ²	300
Thickness, μm	270
Porosity, g/m ³	1
Modulus of elasticity of the paper <i>E</i> , MPa	0.01±0.02×10 ⁵

The results of experimental investigations obtained by exciting the investigated material using vibrations are presented in Fig. 22, ..., Fig. 30.

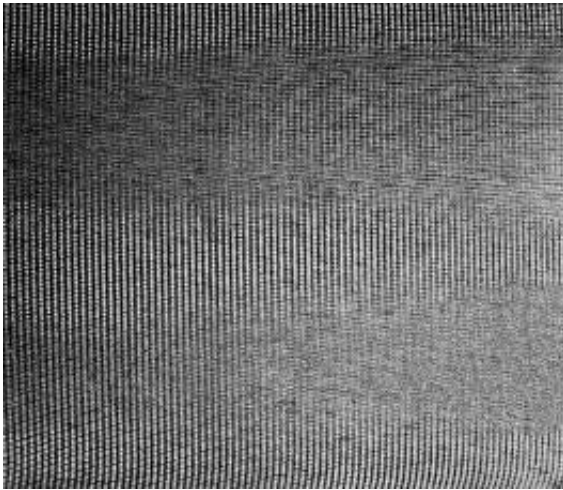


Fig. 22. The first experimental eigenmode: frequency of vibrations 120 Hz, amplitude 8×10⁻⁶m

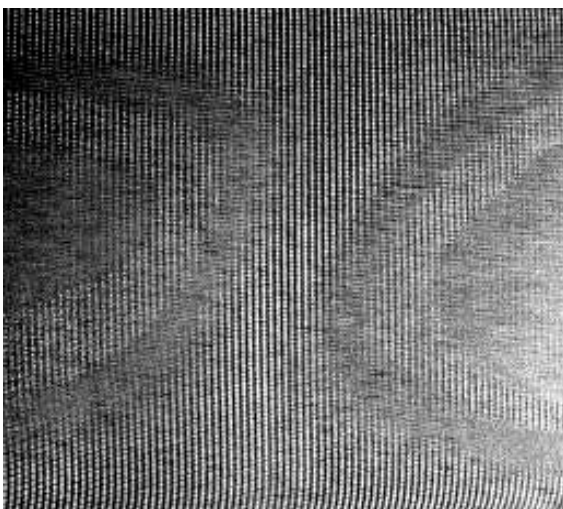


Fig. 23. The second experimental eigenmode: frequency of vibrations 126 Hz, amplitude 8×10⁻⁶m

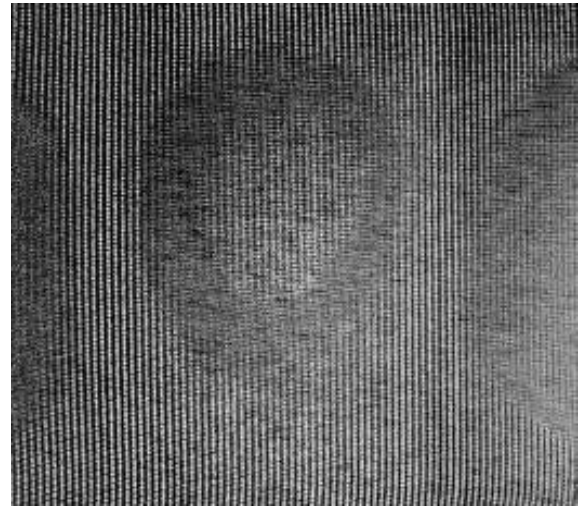


Fig. 24. The third experimental eigenmode: frequency of vibrations 141 Hz, amplitude 8×10⁻⁶m

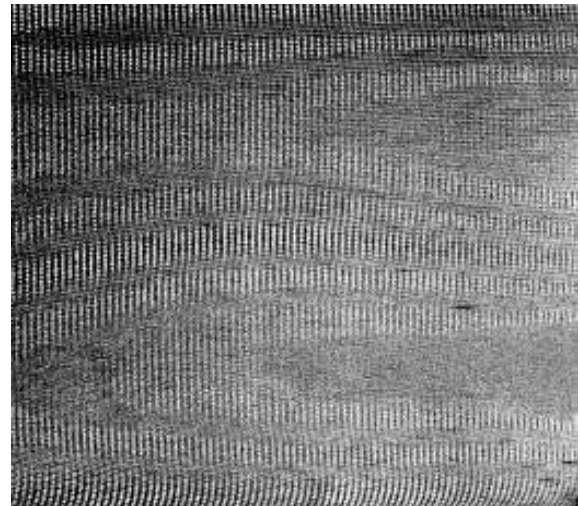


Fig. 25. The fourth experimental eigenmode: frequency of vibrations 244 Hz, amplitude 8×10⁻⁶m

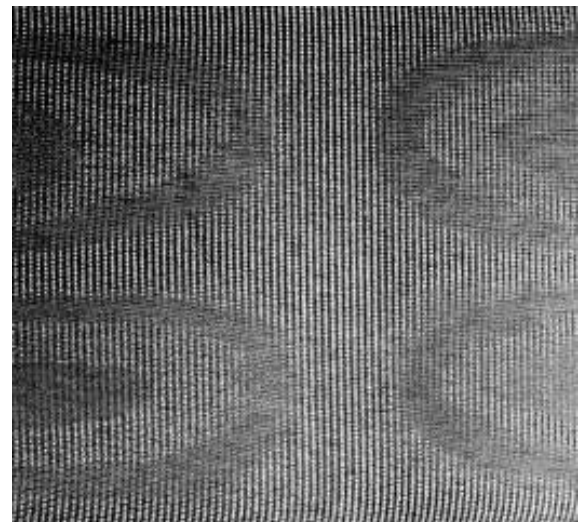


Fig. 26. The fifth experimental eigenmode: frequency of vibrations 277 Hz, amplitude 3×10⁻⁶m

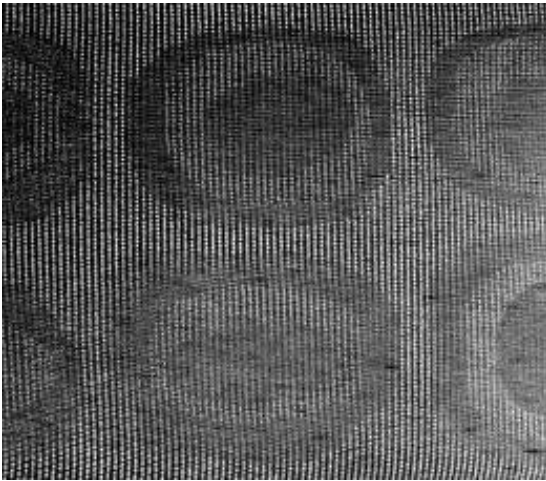


Fig. 27. The sixth experimental eigenmode: frequency of vibrations 297 Hz, amplitude 3×10^{-6} m

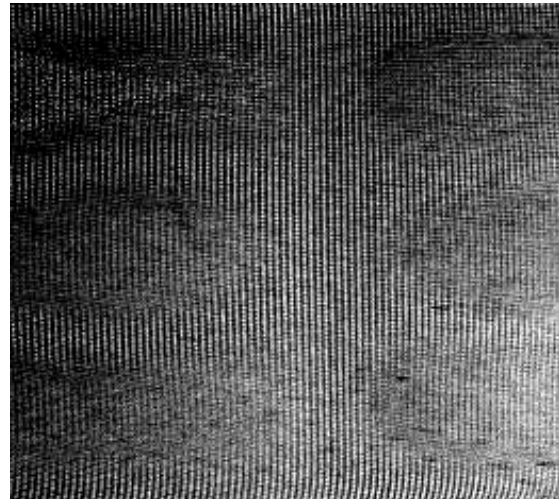


Fig. 30. The ninth experimental eigenmode: frequency of vibrations 430 Hz, amplitude 3×10^{-6} m

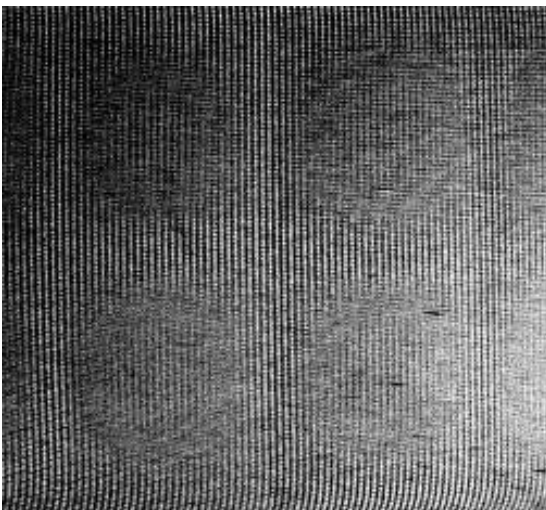


Fig. 28. The seventh experimental eigenmode: frequency of vibrations 342 Hz, amplitude 3×10^{-6} m

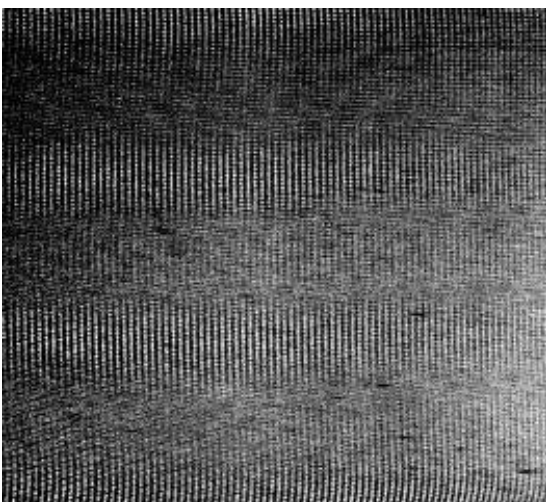


Fig. 29. The eighth experimental eigenmode: frequency of vibrations 410 Hz, amplitude 3×10^{-6} m

Obtained results indicate that the first, the second and the third experimental images (see Fig. 22, Fig. 23, Fig. 24) directly correspond to the numerically obtained first, second and third eigenmodes (see Fig. 12, Fig. 13, Fig. 14). Among the higher eigenmodes one can observe some changes in their sequence, for example the fifth experimental eigenmode (see Fig. 26) corresponds to the numerically obtained ninth eigenmode (see Fig. 20). This is related to the fact that the higher eigenmodes are more sensitive to the physical and geometrical parameters of the structure and to the loading of the structure.

Conclusions

The stress strain law on the basis of the model of a visco-elastic body is used, which enables modal decomposition of the equations of motion by using the eigenproblem of an un-damped system. Results of numerical calculations of vibrations of a visco-elastic structure are presented.

It is assumed that a polymeric film in a printing device is loaded in its plane. The static problem of plane stress by assuming the displacements at the boundary of the analyzed polymeric film to be given is solved. The principal stresses are calculated and represented at the centers of finite elements. They substantially determine the vibration behavior and stability of the polymeric film.

Stresses in the polymeric film in the transverse and longitudinal direction of transportation of the tape were determined by using experimental methods for the symmetric and non-symmetric loads.

After performing the measurements of normal stresses of a polymeric film POP+AL+LDPE for symmetric and un-symmetric loads the values of stresses in the chosen places of the film were determined. Highest stresses were obtained in the central part of the material at the fixing place of the film when the stresses are measured in the direction parallel to the direction of loading.

After performing the measurements of stresses in the direction perpendicular to the direction of loading, much smaller stresses were obtained in comparison to the case when the direction is parallel to the direction of loading.

For un-symmetric loading of the film the distribution of stresses in the region of the polymeric film is not so continuous as in the case of symmetric loading.

The general character of the experimentally obtained field of stresses corresponds to the numerically obtained one. This is evident from the figures presented in the paper and holds true for both symmetric as well as un-symmetric loads.

The analysis of vibrations of a paper in a printing device was performed. For the investigation of the eigenmodes a special experimental setup was used in which the eigenmodes of the paper tape were determined by using the method of projection moire under the action of vibrations to the tape of paper for the symmetric load. Experimental and numerical results of investigation were compared.

In the course of experimental investigations the chalk mate paper Luxo Satin 300 g/m² was excited by longitudinal vibrations of sinusoidal shape of the chosen frequency in the cross-machine direction of paper. The experimentally obtained first several eigenmodes are in good agreement with the numerically obtained ones.

However the discrepancy of results is observed for the case of higher eigenmodes: there are interchanges in the sequence of experimental and numerical eigenmodes. This is explained by the fact that the higher eigenmodes are more sensitive to the changes of the geometrical and physical parameters of the paper and particularly to the static loading of the paper.

The obtained experimental and numerical results are used in the process of design of packages and selection of the materials for their production.

References

1. **Samul V. I.** Basis of the Theory of Elasticity and Plasticity. Moscow: Vysshaja Shkola, 1982.
2. **Bolotin V. V.** Vibrations in Engineering. Handbook. Vol. 1. Moscow: Mashinostroenie, 1978.
3. **Zienkiewicz O. C.** The Finite Element Method in Engineering Science. Moscow: Mir, 1975.
4. **Bathe K. J.** Finite Element Procedures in Engineering Analysis. New Jersey: Prentice-Hall, 1982.
5. **Kibirškis E., Kabelkaitē A., Dabkevičius A., Ragulskis L.** Investigation of vibrations of a sheet of paper in the printing machine. Journal of Vibroengineering. Vol. 9(2), 2007, p. 40-44.
6. **Kabelkaitē A., Kibirškis E., Ragulskis L., Dabkevičius A.** Analysis of vibrations of paper in a printing device. Journal of Vibroengineering. Vol. 9(1), 2007, p. 41-50.